ANL/OTEC-PS-7

OTEC Performance Tests of the Trane Plate-Fin Heat Exchanger

C. B. Panchal, D. L. Hillis, J. J. Lorenz,
and D. T. Yung

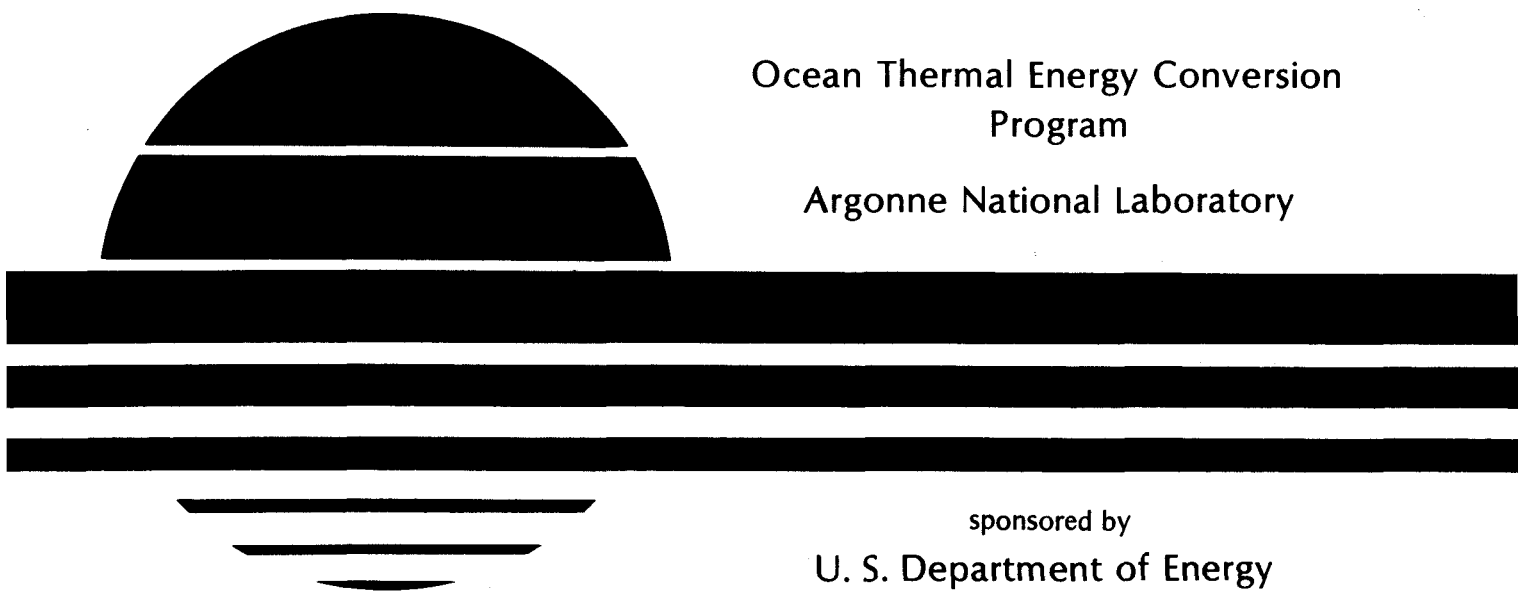

Ocean Thermal Energy Conversion Program

Argonne National Laboratory

sponsored by
U. S. Department of Energy
under Contract W-31-109-Eng-38

The facilities of Argonne National Laboratory are owned by the United States Government. Under the terms of a contract (W-31-109-Eng-38) among the U. S. Department of Energy, Argonne Universities Association and The University of Chicago, the University employs the staff and operates the Laboratory in accordance with policies and programs formulated, approved and reviewed by the Association.

MEMBERS OF ARGONNE UNIVERSITIES ASSOCIATION

The University of Arizona
Carnegie-Mellon University
Case Western Reserve University
The University of Chicago
University of Cincinnati
Illinois Institute of Technology
University of Illinois
Indiana University
The University of Iowa
Iowa State University
The University of Kansas
Kansas State University
Loyola University of Chicago
Marquette University
The University of Michigan
Michigan State University
University of Minnesota
University of Missouri
Northwestern University
University of Notre Dame
The Ohio State University
Ohio University
The Pennsylvania State University
Purdue University
Saint Louis University
Southern Illinois University
The University of Texas at Austin
Washington University
Wayne State University
The University of Wisconsin-Madison

Printed in the United States of America
Available from
National Technical Information Service
U. S. Department of Commerce
5285 Port Royal Road
Springfield, VA 22161

NTIS price codes
Printed copy: A04
Microfiche copy: A01

Distribution Category:
Ocean Thermal Energy
Conversion (UC-64)

ANL/OTEC-PS-7

ARGONNE NATIONAL LABORATORY
9700 South Cass Avenue
Argonne, Illinois 60439

OTEC PERFORMANCE TESTS OF THE TRANE PLATE-FIN HEAT EXCHANGER

by

C.B. Panchal,* D.L. Hillis,* J.J. Lorenz,† and D.T. Yung†

*Energy and Environmental Systems Division
†Components Technology Division

April 1981

The Argonne Ocean Thermal Energy Conversion Program
is a joint effort of the
Energy and Environmental Systems Division
and Components Technology Division

sponsored by

U.S. DEPARTMENT OF ENERGY
Assistant Secretary for Conservation and Renewable Energy
Division of Solar Electric Technologies

CONTENTS

CONTENTS (Cont'd)

FIGURES

TABLES

TABLES (Cont'd)

NOMENCLATURE

OTEC PERFORMANCE TESTS OF THE TRANE PLATE-FIN HEAT EXCHANGER

by

C.B. Panchal, D.L. Hillis, J.J. Lorenz,
and D.T. Yung

ABSTRACT

The Trane heat exchanger was tested as an evaporator, and separately as a condenser, at the following nominal operating conditions: water flow rate, 3200 gpm; heat duty, 3.2 million Btu/h; and ammonia feed rate (applicable to evaporator test only), 26 gpm. Operated as an evaporator in the forced-convection mode, the overall heat-transfer coefficient (U_o) of the unit was 1235 Btu/h·ft^2·°F. The water-side and ammonia-side pressure drops were 3.1 psi and 1.6 psi, respectively. Tests were conducted at heat duties ranging from 2.4 million to 4 million Btu/h, and at ammonia feed rates ranging from 18 to 40 gpm. Over these ranges, U_o did not change more than about 5%. Operated as an evaporator in the falling-film mode, at the same nominal conditions as listed above, U_o was 1035 Btu/h·ft^2·°F. At a constant heat duty, increasing ammonia feed rate from 22 to 50 gpm increased U_o by about 30%. A similar trend was observed when heat duty was increased to 4 million Btu/h. Operated as a condenser, the unit's U_o was 870 Btu/h·ft^2·°F. When the heat duty of the condenser was increased from 2.4 million to 4 million Btu/h, U_o decreased by about 25%.

1 INTRODUCTION

Development of an efficient and cost-effective heat-exchanger system is of prime importance to the Ocean Thermal Energy Conversion (OTEC) program. Improvements in the performance of evaporators and condensers can significantly reduce both capital costs and operating costs. As part of a program to evaluate potential OTEC evaporators and condensers, several heat exchangers, each of them rated at one megawatt thermal (1 MWt), have been tested at Argonne National Laboratory. All of these heat exchangers are sized to handle 3.2 million Btu/h, corresponding to an electricity-generating capacity one-fortieth of that size. (For an OTEC plant's projected operating efficiency of approximately 2.5%, 40 MWt is equivalent to 1 MWe.) Consequently, through these tests it should be possible to determine whether the performance anticipated on the basis of small-scale experiments can be achieved in large configurations. Such information is necessary before full-size commercial OTEC plants can be designed. The initial test series covered seven heat exchangers. The first six units tested were: the Union Carbide flooded-bundle evaporator[1]; the Union Carbide enhanced-tube condenser[2]; the Union Carbide sprayed-bundle evaporator[3]; the Carnegie-Mellon University vertical fluted-tube condenser[4]; the Carnegie-Mellon University vertical fluted-tube evaporator[5]; and the Johns Hopkins University Applied Physics Laboratory (JHU/APL) folded-tube evaporator[6].

The purpose of this report is to present and discuss the results of performance-testing a vertical plate-fin evaporator designed and built by the Trane Company. The Trane evaporator is the first compact-style heat exchanger to be tested at Argonne. (The unit is designated "compact" because its plate-fin design develops higher thermal power per unit of heat-exchanger volume than does a shell-and-tube exchanger design.) Although this particular standard-production unit was not designed for seawater service, similar units with different water-side configuration appear potentially attractive for OTEC applications. The Trane exchanger was first tested as a forced-convection evaporator, the mode of operation for which it was designed. It was later tested as an evaporator in the falling-film mode of operation, and also as a condenser. Additional testing was done with varying amounts of water in the ammonia to determine the effects on performance; these test results are being reported in detail elsewhere[7] and will not be repeated here.

2 PLATE-FIN EVAPORATOR

The Trane plate-fin evaporator used in this testing program is made of 3003 aluminum and consists of alternate water-side and ammonia-side passages brazed together in a sandwich configuration. It is mounted in a vertical orientation. Figure 1 depicts the heat exchanger photographically, Fig. 2 presents its external configuration and dimensions, and Fig. 3 shows its internal serrated-fin arrangement.

In the forced-convection mode of evaporation operation (e_{fc}), liquid ammonia flow is fed in at the bottom of the unit and exits as a two-phase mixture (of approximately 75% quality) at the top. Water is also fed in at the bottom and forced out the top in this mode. In the falling-film mode of evaporator operation (e_{ff}), however, the exchanger was inverted -- with the larger of the two ammonia ports at the bottom of the unit -- and both fluids were fed in at the top. Tested as a condenser the unit was oriented in the same vertical position as that used in forced-convection evaporation. The operating difference between the

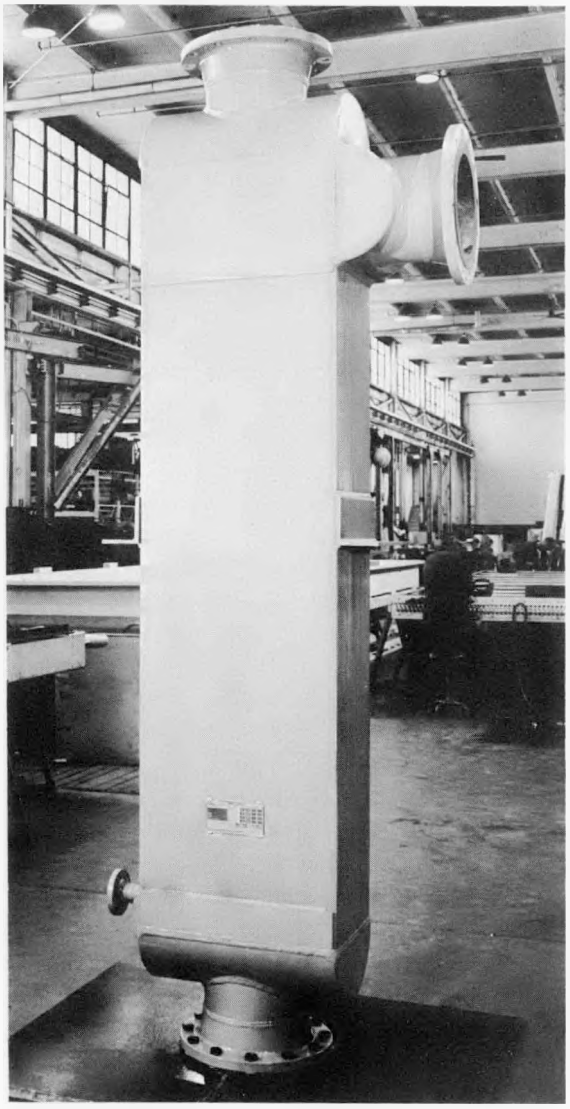

Fig. 1 Trane Plate-Fin Evaporator

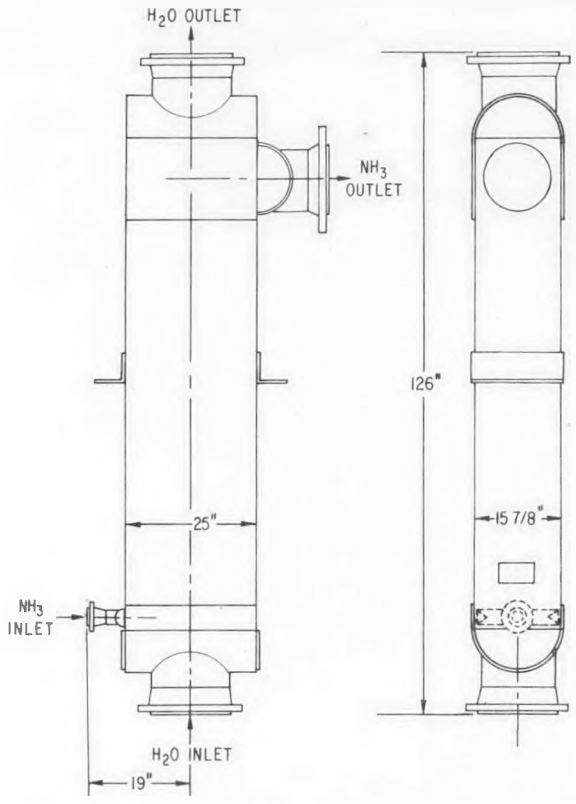

Fig. 2 External Configuration of the Unit (Oriented for e_{fc} Service)

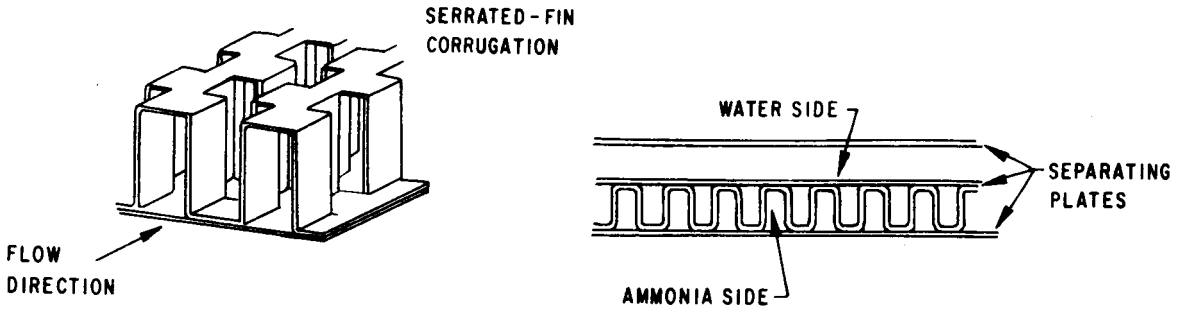

Fig. 3 Two Views of Unit's Internal Configuration, Showing How Serrated Fins are Positioned to Break Up Ammonia Flow through System

unit as a condenser and as a forced-convection evaporator was that in the former, ammonia vapor was fed into the larger ammonia port at the top, exiting as a condensed liquid at the bottom. A standpipe, open to the atmosphere, was installed at the warm-water discharge (the top of the heat exchanger) during two of the tests. The standpipe prevented accidentally overpressurizing the water side during the tests.

The unit's ammonia-side passageway is made up of a series of closely spaced fins to enhance heat exchange. As the left-hand view in Fig. 3 shows, the fins form corrugated surfaces that extend along the flow of the ammonia. This channel arrangement breaks up the boundary layer of the ammonia. The unit's water-side passageway is 0.228 in. by 7.58 in. (0.58 cm by 19.25 cm) -- this provides structural strength, but not water-side enhancement as such.

Table 1 presents nominal design parameters for the unit operated as an evaporator. Although Trane did not design the unit for condensing service, the company has predicted a nominal heat duty of 2.9 million Btu/h for it when it is operated for that purpose.

Table 1 Nominal Parameters for the Plate-Fin Evaporator

Parameter	Value
Heat duty (10^6 Btu/h)	3.2
Water flow rate (gpm)	3200
Water inlet temperature (°F)	80
Water outlet temperature (°F)	78
Ammonia feed rate (gpm)	26
Ammonia feed temperature (°F)	56
Ammonia vapor temperature (°F)	72
Ammonia vapor quality at exit (%)	77
Heat-transfer area[a] (ft^2)	775
Area ratio[b]	3.5
Number of ammonia-side passages	26
Number of water-side passages	27
Water-side enhancement	None
Overall heat-transfer coefficient (Btu/h·ft^2·°F)	627
Water-side pressure drop (psi)	3

[a]Based upon flat-plate water-side area.

[b]Total ammonia-side area divided by flat-plate area.

3 HEAT-EXCHANGER TEST FACILITY

3.1 MECHANICAL COMPONENTS

A piping schematic of the OTEC heat-exchanger test facility at Argonne is shown in Fig. 4. The facility consists of a warm-water loop, a test evaporator, an ammonia loop, a test condenser, and a cold-water loop. It is possible to test evaporator and condenser concurrently; in fact, data are regularly taken for both units during any test run. From an operational standpoint, however, it is not practicable to control operating conditions for both exchangers at the same time. The arrangement shown in Fig. 4 differs from that used to test shell-and-tube units in that the test exchangers are located at the pump suctions, rather than at the pump discharges. The water pumps used in the test loop are high-head centrifugal pumps obtained from government surplus and are not typical of pumps that would be used in an actual OTEC installation. Shell-and-tube exchangers normally have high water-side pressure ratings and thus can be placed anywhere in the loop. The Trane exchanger, on the other hand, has a relatively low water-side pressure rating; it is necessary to locate this unit close to the pump inlet so as to attain adequate pump suction-pressure without overpressurizing the exchanger.

The nominal heat duty for both water loops is 3.2 million Btu/h. Testing was normally done in the range of 2.4-4 million Btu/h. Heat duties as high as 6 million Btu/h are possible, but only with water entering the

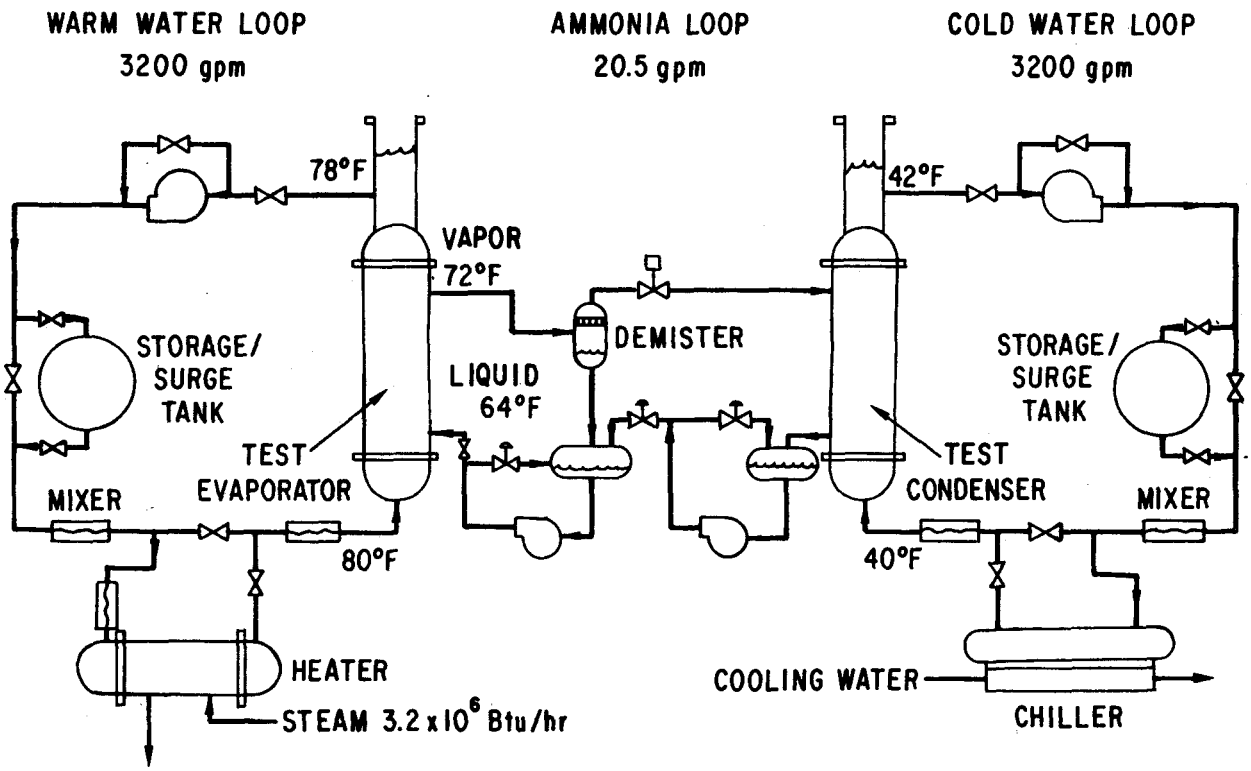

Fig. 4 Piping Schematic of OTEC Heat-Exchanger Test Facility

condenser at a higher temperature. (Higher water temperature at this point leads to higher ammonia temperature and pressure.) The nominal water flow rate for both loops is 3200 gpm. Testing is normally done in the range of 1500-5000 gpm in order to separate the water-side and ammonia-side heat-transfer coefficients using the Wilson-plot method.

The ammonia loop has a demister that removes entrained liquid from the vapor stream. The demister contains a 6"-thick pad woven from polypropylene filaments. The entrained liquid is caught on the pad and returned to the evaporator sump as a liquid stream exiting the bottom of the demister vessel. The manufacturer's rating indicates that all but sub-micron-size particles are caught at the vapor velocities of the tests. For very high vapor qualitites, such as those obtained with shell-and-tube units, the run-off is collected in bulk over a period of time to obtain a measurement of exit quality. Units such as the Trane evaporator have such high run-offs from the demister that the exit quality is calculated from the heat duty and the ammonia feed rate. Turbine flowmeters are installed in the demister return line, but their readings are not used in analysis; we have found that these small turbine flowmeters are easily damaged by dirt and by two-phase flow, and cannot be depended upon to give reliable readings in this service.

3.2 INSTRUMENTATION

Pressures, temperatures, and flow rates are measured in each of the three test-facility loops (warm water, ammonia, and cold water). The instruments used were chosen on the basis of measurement accuracy and compatibility with the computerized data-handling system. The original accuracy goals for measurements characterizing overall performance of the heat exchangers were ±3% for the overall heat-transfer coefficient and ±5% for the water-side pressure drop. Our best judgment (see Sec. 4.2 below) is that the goal for the overall heat-transfer coefficient has been exceeded. Accurate and reliable measurement of the water-side pressure drop has proved to be a more difficult goal to achieve.

Six quartz-crystal thermometers are used for temperature measurements: four to measure water-side temperature changes through the evaporator and the condenser, and two to measure ammonia-side temperatures. For the Trane tests, the two ammonia-side thermometers were installed in the ammonia inlet and exit lines, one in each line. On the basis of the manufacturer's data sheets and our own measurements, we estimate the accuracy of these instruments to be within ±0.02°F. Thermocouples are also used to back up the quartz-crystal instruments and to provide temperature measurement for other parts of the system.

Four quartz-crystal transducers are used to measure ammonia-side pressures -- two at each of the paired heat exchangers (evaporator and condenser) in the system, one at the ammonia inlet and one at the exit. These transducers have a rated accuracy of ±0.005 psia, or ±0.002°F in terms of ammonia saturation temperatures. Since we have no way of calibrating them short of returning them to the manufacturer, we conservatively use a value of ±0.01°F in the error analysis. (Rough checks are routinely made by opening all units to atmosphere to see that they read the same.) Additional pressure-sensing instrumentation, for backup purposes in the ammonia loop, is provided by strain-gage transducers.

Water and ammonia flow rates are measured by turbine flowmeters. The 12-inch meters used in the water loops have a rated accuracy of 0.15% of reading. Although we have no practical means of verifying this figure, we have no reason to believe it has changed over time. Moreover, any serious error in the larger meters would be detected by comparing evaporator and condenser heat duties, which should be equal, ±1%. The turbine meters used in the ammonia liquid lines have a claimed accuracy of ±0.5% of reading. As noted above, these are susceptible to damage; in practice, however, the readings are used only to calculate exit quality or reflux ratio, whichever is appropriate. The larger meters used in the ammonia-feed line have proved more rugged and reliable than the smaller meters used in the demister-return lines.

Water-side pressure drops are measured with strain-gage transducers, which have a rated accuracy of ±0.5% of reading. Although this is sufficiently accurate for the purpose, installing them in a manner to produce meaningful and repeatable readings has proved to be difficult in practice. The usual method is to examine many readings, discard those that appear either much too high or much too low, and average the rest. It is impossible to state with certainty that this technique results in the desired accuracy of ±5%. However, when this procedure is applied to pressure drops over a wide range of water flow rates, the values are proportional to the square of the flow rates within a few percent, as would be expected.

3.3 DATA-HANDLING SYSTEM

The test facility has a computerized data-acquisition system that can read the sources of data, apply calibration and correction factors to these data, compute heat balances and overall heat-transfer coefficients, and produce hard-copy and magnetic-tape records of all measured and calculated quantities. After completing tests of the five shell-and-tube heat exchangers, the data-handling program was completely rewritten to accommodate the special requirements of the JHU/APL folded-tube evaporator, which was tested early in 1979. This same basic program has been used for all tests since then. The new program differs from the old in that it automatically samples all the data periodically at a rate determined by the operator (generally four to five times per minute); keeps a running average of the various data; and, after a given number of data sets (usually 20 or 30), prints out the average measured values and the calculations based upon them. All data, including the instantaneous sampled measurements, can be stored on magnetic tape. Needless to say, this produces a vast number of printouts. The usual practice is to use only the last three printouts, representing perhaps 60 data sets, for each set of operating conditions.

3.4 OPERATING PROCEDURE

Because of the relatively low water-side pressure rating of the Trane (and also the JHU/APL) exchanger, installation reqiuirements for this unit differed from those of the shell-and-tube units tested earlier. For the initial tests as a forced-convection evaporator, the Trane unit was installed near the warm-water pump suction and adjacent to the JHU/APL folded-tube evaporator. The latter unit was tested alternately with the Trane heat

exchanger over a period of several months. For testing as a condenser, the exchanger was moved to the opposite end of the facility, near the suction of a second cold-water pump installed for the sole purpose of testing the Trane and JHU/APL evaporators as condensers. As noted above, a standpipe was used in both installations to limit water-side pressures. For testing as a falling-film evaporator, the unit was moved to a third, intermediate location. In the falling-film test, the standpipe was eliminated and pressures controlled by careful throttling of the warm-water loop. Each time the unit was moved from one installation to another, the ammonia piping was checked for leaks. This was done with nitrogen under pressure after a soap solution (Snoop) had been applied around the new joints. Testing and any necessary repair procedures were also conducted after ammonia was put into the system. (Ammonia leaks are very easy to find.)

The first step in any startup is to evacuate the ammonia system, primarily to remove water vapor. This is done three times at a pressure of about 300 μm as measured at the vacuum pump. The system is back-filled with dry nitrogen after the first two pumpdowns, and with ammonia vapor after the third pumpdown. Liquid ammonia is then forced into the system under pressure to fill the evaporator and condenser receivers to the desired levels. Additional ammonia inventory in the system is usually required after startup -- a typical test inventory is about 600 gallons. The ammonia pumps are started and circulation established through the receivers. Next in order of starting are the cold-water pump, the chiller, and the warm-water pump. Water flow rates are adjusted in both loops (usually to the nominal value of 3200 gpm), and the chiller temperature is set to the desired value. Ammonia flow to the evaporator is started and set to the desired value. The expansion valve is also set to maintain the desired evaporator pressure, generally 133 to 134 psia. The last thing to be turned on is the steam heater for the warm-water loop; by the time ammonia is introduced into the evaporator, the warm-water-loop temperature is already above the desired operating level because of the heat added by the pump work. The condenser is routinely vented during operation to remove any noncondensables that may have accumulated.

In testing evaporators, the parameters that are held constant during a given test run are warm-water flow rate, ammonia feed rate, heat duty, and evaporator pressure; the water temperature is allowed to reach its equilibrium value in the closed loop. In condenser testing, the constant parameters are cold-water flow rate, heat duty, and cold-water temperature -- here, condenser pressure is the free variable. In both cases, heat duty is controlled from the evaporator side. The choice of this method of test control is based upon the following considerations: (a) it results in the most stable operation of the facility; (b) the Wilson-plot method assumes a constant heat flux; (c) it takes a long time for the loop to regain steady-state conditions after a change in heat duty; and (d) it is easy to control cold-water temperature but impractical to try to control condenser pressure.

The facility was designed so that all test parameters except flow rates could be controlled automatically. In practice, manual control generally results in more stable operation. Heat duty is always controlled manually. Control of evaporator pressure and cold-water temperature can be either manual or automatic; this is an "operator's choice," often depending upon how well the automatic controllers happen to be working at the time. Although the nominal cold-water temperature is 40°F, most testing is actually done at about 41°F because chiller operation is more stable at the higher temperature.

After the test parameters have been set, it usually takes two to four hours before steady-state operation is reached. Steady-state conditions are signalled by a "leveling off" of one of the dependent variables, either warm-water temperature (for evaporators) or overall heat-transfer coefficient (evaporators or condensers). Data are taken continuously during the test run. After usable data are obtained, the test parameters are changed and the cycle repeated. The tests are scheduled so that heat duty is changed as infrequently as possible. Under ideal conditions, the facility is started up on a Monday morning and run continuously until Friday afternoon, for a total of about 100 hours of operation. After completion of a week's run, the loop is shut down in approximately the reverse order of that used during startup, and the ammonia is transferred to storage tanks located outside the building. For reasons of safety, ammonia is not left in the facility when it is unattended.

There were no operational problems resulting from the characteristics of the Trane heat exchanger. Operation was stable, and results were consistently repeatable.

4 METHODS OF CALCULATION

4.1 HEAT DUTY

As described in earlier reports (e.g., Ref. 5), the heat duty, q, can be determined in several ways. However, the most accurate measurement comes from calculating the rate at which heat is given up by the water as it passes through the heat exchanger. This can be expressed as

$$q = m \cdot C_p \cdot \Delta T \tag{1}$$

The frictional heat generated in the heat exchanger is less than 0.5% of q and is not considered in the calculation. Temperature difference, ΔT, is measured directly; the measurement error is about 0.01°F, while the uncertainty in the water flow rate is 0.15% of reading. Thus, the estimated uncertainty in the calculated heat duty at nominal conditions is 0.5%.

4.2 OVERALL HEAT-TRANSFER COEFFICIENT

The overall heat-transfer coefficient, U_o, is calculated from the conventional definition

$$U_o = \frac{q}{A_o \, \Delta T_{lm}} \tag{2}$$

where:

A_o = reference-heat-transfer area (smooth water-side area in the present case)

ΔT_{lm} = log-mean temperature difference

In the above equation, ΔT_{lm} can be expressed as

$$\Delta T_{lm} = \frac{T_i - T_o}{\ln\left[\frac{T_i - T'}{T_o - T'}\right]} \tag{3}$$

where:

T_i, T_o = water inlet and outlet temperatures, respectively

T' = mean saturation-temperature of ammonia

Combining Eqs. 2 and 3 gives

$$U_o = \frac{m \cdot C_p}{A_o} \ln\left[\frac{T_i - T'}{T_o - T'}\right] \tag{4}$$

The uncertainty in U_o is due in part to inaccuracies in measurements of T_i and T_o obtained with quartz-crystal thermometers. These inaccuracies arise from the inherent precision limits of the thermometers and from errors introduced during calibration. The quartz-crystal thermometers are individually calibrated by the manufacturer (Hewlett Packard), and each one is supplied with a calibration module. These thermometers are regularly adjusted at ANL at a fixed, known temperature to correct for possible drift. The standard procedure is to place the measuring probes in a slush of ice made from distilled water. The readings are allowed to stabilize, and each probe is adjusted to read 0°C. This procedure is followed regularly before starting to take data from a particular heat exchanger. Any resulting measurement error is estimated to be no greater than 0.02°F.* The error in T' resulting from a 0.005 psi uncertainty about pressures measured at the ammonia inlet and ammonia outlet is in the range of .002°F. However, pressure transducers are not calibrated or adjusted regularly at ANL, and hence a conservative value of 0.01°F is taken in the present case. The uncertainty in U_o is the combined effect of the flowmeter uncertainty (0.15%) and three sources of uncertainty because of possible errors in T_i, T_o, and T'. These error components are independent of one another, and thus the estimated uncertainty in Uo is about 1.5% at nominal conditions.

4.3 INDIVIDUAL HEAT-TRANSFER COEFFICIENTS

The heat exchanger is not instrumented for measuring individual ammonia-side and water-side heat-transfer coefficients; however, those coefficients can be determined by means of the standard Wilson-plot procedure. A Wilson plot makes use of the relationship between U_o and the individual coefficients: it expresses the total heat-transfer resistance as the sum of its separate components. For a compact heat exchanger, this can be expressed as the equation

$$\frac{1}{U_o} = \frac{A_o}{h_i A_i} + \frac{1}{h_o} + R_w + R_{fo} + \frac{A_o}{A_i} R_{fi} \qquad (5)$$

It should be pointed out that the ammonia-side heat-transfer coefficient varies along the length of the heat exchanger depending upon the local conditions. Consequently, the h_o value in the above equation represents an average value over the entire length of the heat exchanger. Furthermore, it is known that the water-side coefficient, h_i, varies proportionally to the β power of the water flow rate. However, experimental data for the heat transfer in compact heat exchangers are scanty, making the value of not easily available. In the present work, therefore, a set of values of power index β was tried and the value 0.83 (according to the Kays-London equation) was settled on for h_i.

Clearly, the use of this procedure for determining h_o and h_i required that the data on U_o be obtained under conditions where h_o is constant at different water flow rates and the power index for the water-side coefficient is known. Furthermore, the fouling-resistance factors R_{fo} (ammonia side) and

---

*This is an absolute error; the ΔT error is less because some of the sources of the absolute errors cancel out in the electronics.

R_{fi} (water side) should be known. It is expected that if the heat duty and ammonia feed rate are kept constant, h_o will also remain constant while water flow rates are varied. Although the ammonia pressure remained constant from run to run, it was necessary to vary water inlet temperature in order to maintain constant heat duty. As a result of different water flow rates at constant heat duty, local differences are created between the wall temperature and ammonia saturation temperature along the length of the heat exchanger. Nevertheless, the average ammonia-side coefficient, h_o, remains relatively constant because the inlet and outlet conditions for the ammonia side are maintained constant.

In summary, the Wilson-plot procedure cannot be very accurate for determining individual heat-transfer coefficients for heat transfer with phase change. However, meaningful results can be obtained if an accurate power index for the water-side coefficient is known. In the present study, therefore, this procedure is used to determine individual coefficients at nominal conditions only in order to know their relative values.

5 TEST RESULTS

The Trane heat exchanger was tested in three different ways: as an evaporator in the forced-convection mode, as an evaporator in the falling-film mode, and as a condenser. The test data analyzed here are tabulated in the Appendixes. Each mode of operation is analyzed separately. The test results arrived at experimentally are compared with the theoretical model of Yung et al.[8] in Sec. 7.

5.1 EVAPORATOR IN FORCED-CONVECTION MODE

5.1.1 Performance at Nominal Operating Conditions

The nominal operating conditions for the Trane evaporator are: a water flow rate of 3200 gpm, a heat duty of 3.2 million Btu/h, and a liquid-ammonia feed rate of 26 gpm. At these conditions, the heat flux was about 4100 Btu/h·ft^2; the exit quality of the ammonia, 77%. The overall heat-transfer coefficient at nominal conditions was 1235 Btu/h·ft^2·°F, reproducible to within 1%. There was no apparent operational problem while thermohydraulic performance of the evaporator was consistent and stable. Individual heat-transfer coefficients, using the Wilson-plot technique, were backed out from the overall value for the water side and amonia side. The water-side coefficient thus determined was 1770 Btu/h·ft^2·°F.* The ammonia-side coefficient was 4085 Btu/h·ft^2·°F.* The water-side and ammonia-side pressure drops were, respectively, 3.1 psi and 1.7 psi. Figure 5 shows the effect of water flow rate on the overall heat-transfer coefficient. Table 2 presents the data on which Fig. 5 is based. A 77% exit quality is constant for all results in Table 2.

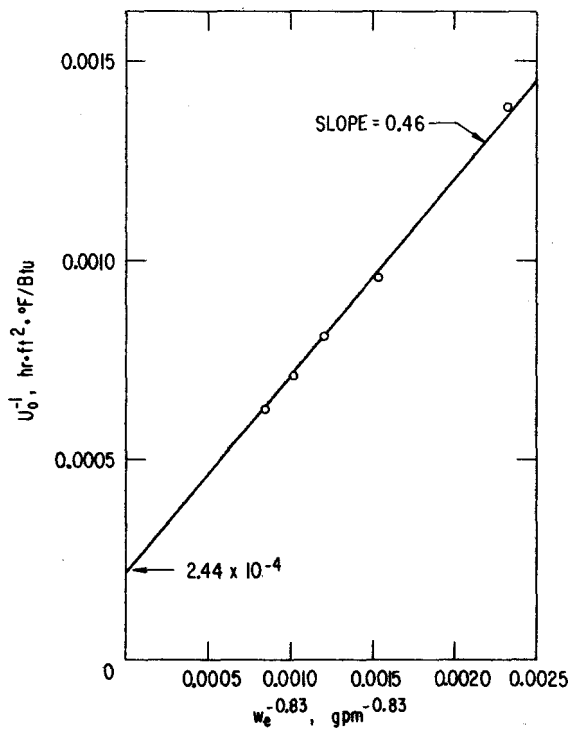

Fig. 5 Evaporator Performance at Nominal Operating Conditions: Forced-Convection Mode

*The ammonia-side and water-side coefficients reported by ANL earlier[9] are different from those reported here. A power index of 0.8 was originally used in the Wilson plot. Later it was determined that a power index of 0.83, the value used here, is more appropriate for the Trane heat exchangers. The power-index value and the value referred to in Sec. 4.3 of this report are identical.

Table 2 Overall Heat-Transfer Coefficient as a Function of Water Flow Rate: Evaporator, Forced-Convection Mode

Water Flow Rate[a] (gpm)	Heat Duty (10^6 Btu/h)	Ammonia Flow Rate (gpm)	Overall Heat-Transfer Coefficient (Btu/h·ft^2·°F)
3249	3.24 ± 0.13	25.6 ± 0.1	1235
2391			1040
3996			1405
5043			1590
1482			760
3203	4.02 ± 0.16	33.2 ± 0.1	1255
4015			1410
5012			1555
2407			1065
1502			785

[a]These values can be converted to mean-flow velocity (v in ft/sec) using the relationship $v = 0.00233\ w_e$.

5.1.2 Effects of Ammonia Feed Rate and Exit Quality

Keeping the water flow rate essentially constant, tests were conducted to study the ammonia-side heat-transfer performance as a function of ammonia feed rate and heat duty. In the case of forced-convection vaporization, the heat-transfer coefficient is, in general, a function of the ammonia feed rate, mass quality, and thermophysical properties.

In Fig. 6, the overall heat-transfer coefficient is plotted against ammonia vapor quality at exit, with ammonia feed rate as a parameter. The limited number of data points used in preparing the plot are joined together according to different ammonia feed rates. A broken-line curve is used where the trend is not absolutely clear from the test results. It should be noted in Fig. 6 that the heat-transfer coefficient was very low for a 31% exit quality. A slight drop in performance was observed, as well, when the exit quality exceeded 90%. This latter drop indicates a possible drying out in a part of the heat exchanger, probably near the exit region.

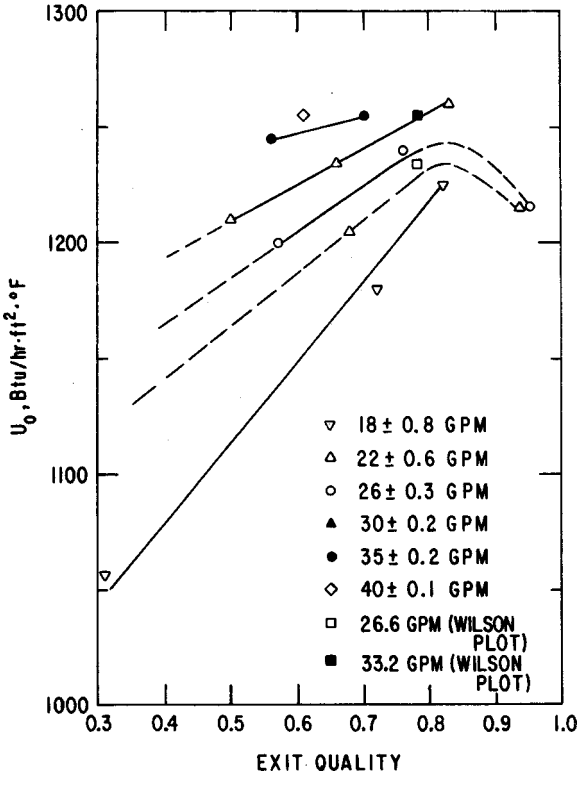

Fig. 6 Evaporator Performance for Various Ammonia Feed Rates, as a Function of Ammonia Exit Quality: Forced-Convection Mode

The same data used in Fig. 6 are cross-plotted in Fig. 7. There, the overall coefficients are plotted against the total ammonia feed rate, with ammonia exit quality as a parameter. The two broken lines in Fig. 7 indicate the upper and lower boundaries of experimental error. Most of the data points lie within the boundary limits. A similar observation was made by Robertson[10] for the convective evaporation of nitrogen in a serrated-fin channel. He observed that the heat-transfer coefficient is relatively insensitive to a mass flux below 22,000 lb/h·ft^2 and an exit quality below 80%. In the present study, the mass flux ranged between 9,000 lb/h·ft^2 and 12,000 lb/h·ft^2.

Figures 6 and 7 lead to the general conclusion that the heat-transfer coefficent does not change significantly as a result of changes in ammonia feed rate or its vapor quality exiting the heat exchanger. The overall heat-transfer coefficient does not change more than about 10% when ammonia feed rate is changed from 17 to 40 gpm or exit quality is changed from 50% to 95%.

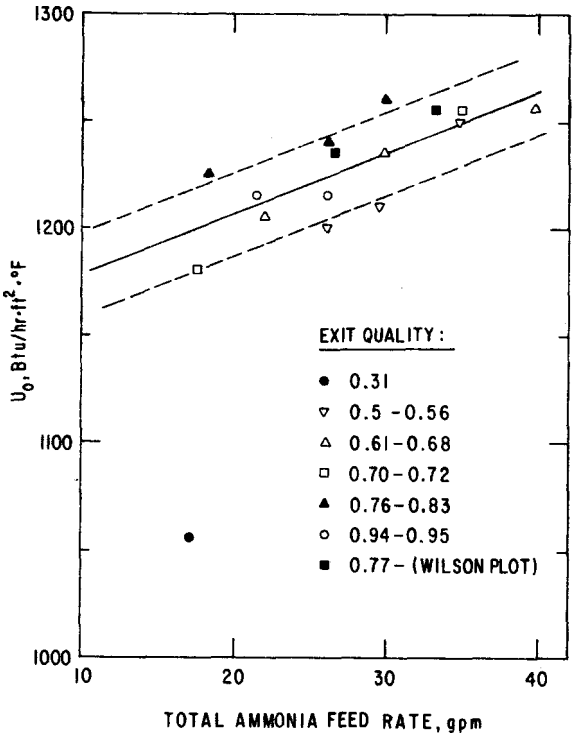

Fig. 7 Evaporator Performance for Various Ammonia Exit Qualities, as a Function of Ammonia Feed Rate: Forced-Convection Mode

5.2 EVAPORATOR: FALLING-FILM MODE

5.2.1 Peformance at Nominal Operating Conditions

Since the Trane heat exhanger was not designed to operate in a falling-film evaporative mode, nominal operating conditions are not defined. If we assume the same nominal conditions as those defined for the forced-convection mode (heat duty of 3.2 million Btu/h, water flow rate of 3200 gpm, and liquid-ammonia feed rate of 26 gpm), the heat flux is about 4100 Btu/h·ft^2 and the recirculation ratio (σ) is approximately 0.30.

The overall heat-transfer coefficient at the above conditions is 1035 Btu/h·ft^2·°F, reproducible to within 2%. There were no apparent starting or operational problems in operating the Trane heat exchanger in the falling-film mode. Individual heat-transfer coefficients are backed out using the Wilson-plot technique. The water-side heat-transfer coefficient is 1755 Btu/h·ft^2·°F; the composite ammonia-side coefficient is 2525 Btu/h·ft^2·°F. The water-side and ammonia-side presure drops are 3.1 psi and 0.4 psi, respectively. Table 3 shows the effects of water flow rate on the overall heat-transfer coefficient for three combinations of heat-duty and ammonia-feed-rate

Table 3 Overall Heat-Transfer Coefficient as a Function of Water Flow Rate: Evaporator, Falling-Film Mode

Water Flow Rate[a] (gpm)	Heat Duty (10^6 Btu/h)	Ammonia Flow Rate (gpm)	Recirculation Ratio	Overall Heat-Transfer Coefficient (Btu/h·ft^2·°F)
3216	3.22 ± 0.5	25.4 ± 1.1	0.23	1035
4017				1140
5027				1225
2403				890
1501				670
3201	4 ± 0.05	33.0 ± 0.3	0.30	1160
3996				1300
4999				1450
2401				1005
1498				745
3198		25.5 ± 0.3	0.01	990
4020				1110
5017				1210
2403				865
1518				645

[a]These values can be converted to mean flow velocity (v in ft/sec) using the relationship $v = 0.00233\ w_e$.

values. Corresponding recirculation ratios were 0.30 and 0.01, respectively. Figure 8 is plotted from data in Table 3.

Table 3 shows the overall heat-transfer coefficient (with recirculation ratio kept constant) at a given water flow rate increases by about 12% when the ammonia feed rate is increased from 25 gpm to 33 gpm. The corresponding increase for the forced-convection mode was about 1.5%. This indicates that the liquid ammonia is not able to wet the surface completely at a low feed rate. It was also observed that the heat-transfer coefficient decreases as ammonia feed rate at constant heat duty increases.

5.2.2 Effects of Recirculation Ratio

The heat-transfer coefficient for the Trane unit employed as a falling-film evaporator is, in general, a function of film Reynolds number and

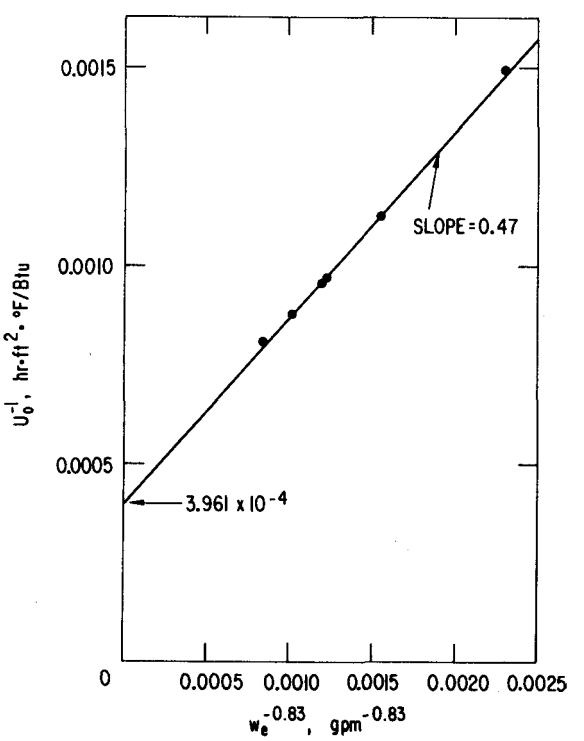

Fig. 8 Evaporator Performance at Nominal Operating Conditions: Falling-Film Mode

interfacial shear caused by the vapor flow. Thus, the ammonia-side coefficient is a function of recirculation ratio and heat duty. According to Nusselt's analysis, the ammonia-side coefficient should decrease as the recirculation ratio increases. The liquid-phase flow regime for the falling-film mode is laminar. However, it is highly probable that, for a complex geometry like the Trane heat exchanger, the liquid is not uniformly distributed over the surface. As a result of uneven liquid distribution, the heat-transfer coefficients deteriorate in two ways: (a) a part of the heat exchanger becomes dry; and (b) liquid film becomes thicker in the area where most liquid tends to flow. Increasing the recirculation ratio of ammonia improves condition (a) but makes condition (b) worse. The net result of the increase, however, is to improve the overall heat-transfer coefficient -- as Fig. 9 indicates.

In Fig. 9 the overall coefficient, U_o, is plotted against recirculation ratio, σ, with heat duty as a parameter. The heat-transfer coefficient increases with recirculation ratio and reaches an asymptotic value. This indicates that at a low recirculation rate not all heat-transfer surfaces are completely wetted with liquid ammonia; dryer surfaces are assumed to be near the exit region. It is observed that for a given recirculation ratio, U_o for 4 million Btu/h heat duty is greater than that for 3.2 million Btu/h heat duty. This is probably because the former produces a thinner film on the heat-exchange surfaces and because the higher vapor flow induces a greater vapor shear. The nature of the curve, however, remains the same at both heat duties.

Finally, the test runs at nominal ammonia feed rates were repeated in order to investigate possible hysteresis effects. It was observed that U_o is not affected by the history of the operational conditions. In summary, the following conclusions can be drawn.

- At low recirculation rates, the heat-transfer surfaces are not completely wetted.
- The heat-transfer performance improves as recirculation ratio, σ, is increased. The overall heat-transfer coefficient increases by about 30% when recirculation ratio is increased from 0.1 to 1.5. (The nominal σ for this heat exchanger is 0.3.)
- Hysteresis effects are negligible, and U_o is reproducible to within 2%.

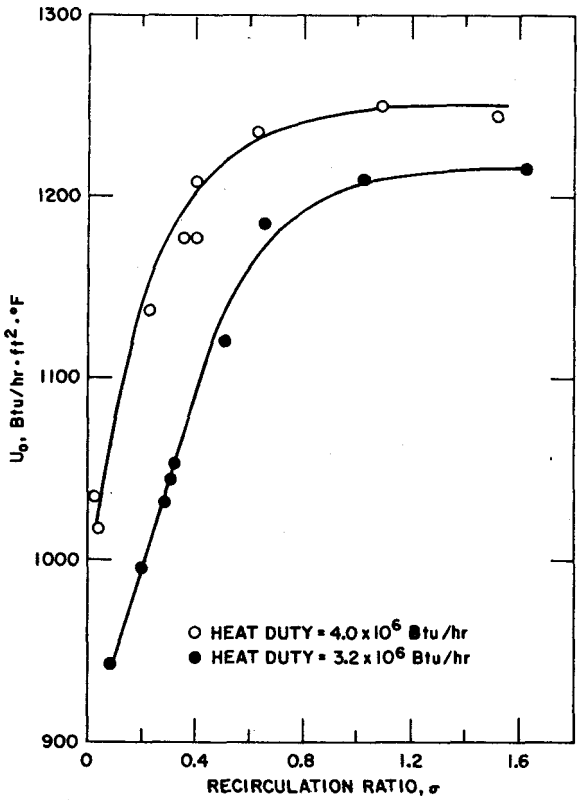

Fig. 9 Evaporator Performance as a Function of Recirculation Ratio: Falling-Film Mode

5.3 COMPARISON OF THE TWO MODES OF EVAPORATOR OPERATION

In a forced-convection evaporator, gravity and friction work in the same direction, causing an appreciable ammonia-side pressure drop through the system. A falling-film evaporator does not have the same drawback, and its pressure drop is less significant. This enables a falling-film evaporator to achieve greater average-temperature driving force -- for the same set of water and ammonia inlet conditions -- than is possible for a forced-convection evaporator. Therefore, if the overall heat-transfer coefficient is the same for the two modes of operation, the falling-film mode yields the higher heat duty and more efficient heat transfer. That coefficient could be different for the two modes, however, even when inlet conditions are the same.

The difference is explained by the surface-wetting pattern of the falling-film mode. As discussed in the previous section, the mode does not permit liquid ammonia to wet the heat-transfer surface completely at low ammonia feed rates. This results in a performance inferior to that of an evaporator operated in the forced-convection mode, where the liquid ammonia is expected to distributed more uniformly under the action of interfacial shear. Moreover, the liquid-distribution system may not provide an equal amount of liquid ammonia to all channels. In Fig. 10, evaporative performances of the two modes of operation are compared at essentially the same heat duty, water flow rate, and ammonia feed rate. It is observed that at low ammonia feed rates U_o for the falling-film mode is very low compared to that for the forced-convection mode. However, this improves at high ammonia feed rates; at those feed rates, U_o for the falling-film mode becomes nearly equal to U_o for the forced-convection mode. An earlier section demonstrated that the heat-transfer coefficient for forced-convection evaporation does not change significantly with ammonia feed rates in the range studied here.

Table 4 presents a comparison of the two modes. The ammonia-side heat-transfer coefficients shown in the table were calculated using the water-side coefficient obtained from the Wilson plot. They represent a means of comparing the effects of ammonia feed rate on the two modes of evaporative operation.

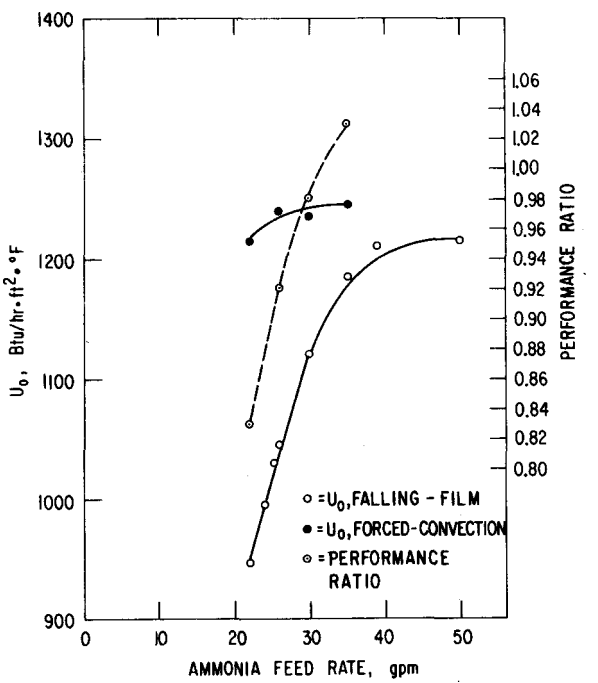

Fig. 10 Performance Ratio (Broken Line) and Comparative Heat-Transfer Coefficients (Solid Lines) for the Two Modes of Evaporative Operation: Falling-Film, Forced-Convection

The two evaporative modes were not compared by measuring their respective heat duties at identical inlet conditions. However, the log-mean temperature of each mode was calculated for a set of identical inlet conditions and experimentally observed

Table 4 Comparison of Evaporator Performance in the Forced-Convection and Falling-Film Modes[a]

Test No.	Heat Duty (10^6 Btu/h)	Ammonia Feed Rate (gpm)	Overall Heat-Transfer Coefficient (Btu/h·ft^2·°F)		Ammonia-Side Heat-Transfer Coefficient (Btu/h·ft^2·°F)		Ratio of Log Mean Temperature: Falling-Film/ Forced Convection	Performance Ratio[b]: Falling-Film/ Forced-Convection
			Forced-Convection Mode	Falling-Film Mode	Forced-Convection Mode	Falling-Film Mode		
1	3.2	22	1250	945	3900	2020	1.07	0.83
2	↓	24	c	995	c	2275	c	c
3		25	c	1030	c	2475	c	c
4		26	1240	1045	4145	2545	1.10	0.92
5		30	1235	1120	4070	3055	1.08	0.98
6		35	1245	1185	4225	3590	1.08	1.03
7		39	c	1210	c	3820	c	c
8	↓	50	c	1215	c	3890	c	c
9	4.0	26	1215	1015	3900	2375	1.08	0.90
10	↓	30	1260	1135	4405	3185	1.07	0.96
11		35	1255	1175	4305	3515	1.06	0.99
12		40	1255	1235	4320	4090	1.05	1.03
13		50	c	1250	c	4260	c	c
14	↓	61	c	1245	c	4190	c	c

[a]A constant water flow rate of 3223 ± 34 gpm, and a constant water-side heat-transfer coefficient of 1770 Btu/h·ft^2·°F, characterized all tests reported here.

[b]Peformance ratio is defined as heat duty in the falling-film mode divided by heat duty in the forced-convection mode -- for the same inlet water temperature, water flow rate, and outlet ammonia pressure.

[c]Not determined.

ammonia-side pressure drops. Table 4 shows that the log-mean temperature of the falling-film mode runs 5-10% higher than that of the forced-convection mode. The product of the heat-transfer coefficient ratio of the two modes and log-mean-temperature ratio of the two modes yields the relative performance of the Trane unit in its two evaporative modes. This performance ratio can be expressed as the following equation.

$$\frac{Q_{ff}}{Q_{fc}} = \left(\frac{U_{o_{ff}}}{U_{o_{fc}}}\right)\left(\frac{\Delta T_{lm_{ff}}}{\Delta T_{lm_{fc}}}\right) \tag{6}$$

where:

Q = performance

ff = falling-film evaporative mode

fc = forced-convection evaporative mode

U_o = heat-transfer coefficient

ΔT_{lm} = log-mean temperature difference

Figure 10 shows that the performance ratio of the falling-film mode divided by the forced-film mode divided by the forced-convection mode is <1 at low ammonia feed rates -- but that it increases as ammonia feed rate is increased and becomes >1 at an ammonia feed rate of about 32 gpm. Nevertheless, no significant improvement in the performance ratio of the evaporator in the falling-film mode is observed.

In summary, the following conclusions can be drawn from the present set of results.

- The overall performance of the Trane evaporator in the falling-film mode is better than that in the forced-convection evaporative mode when the ammonia feed rate is sufficiently high to wet all of the heat-transfer surfaces.
- Both modes of operation are stable and give consistent results. However, U_o can change significantly with ammonia feed rates for the falling-film mode. On the other hand, U_o for the forced-convection mode of operation is insensitive to the ammonia feed rates.

5.4 CONDENSER

5.4.1 Performance at Nominal Operating Conditions

Although the Trane heat exchanger was not designed to operate as a condenser, the manufacturer estimates a condensing-service heat duty of approximately 2.9 million Btu/h at nominal conditions and a water flow rate of 3200 gpm. However, data were taken at 3.2 million Btu/h rather than 2.9 million Btu/h because it was expected that performance would not be significantly different for the two heat duties. At 3.2 million Btu/h, the rate of condensation was about 6258 lb/h.

The overall heat-transfer coefficient at 3.2 million Btu/h heat duty and 3200 gpm water flow rate was 870 Btu/h·ft^2·°F, reproducible to within about 1%. Individual heat-transfer coefficients are backed out using the Wilson-plot technique, and are represented in Fig. 11 and Table 5.

The water-side coefficient (h_i) is 1070 Btu/h·ft^2·°F; the composite ammonia-side coefficient (h_o'), including wall resistance, is 4600 Btu/h·ft^2·°F. The overall heat-transfer coefficient at the rated heat duty of 2.9 million Btu/h would be about 900 Btu/h·ft^2·°F. The water-side pressure drop measurement was not taken; however, the ammonia-side pressure drop was found to be negligibly small.

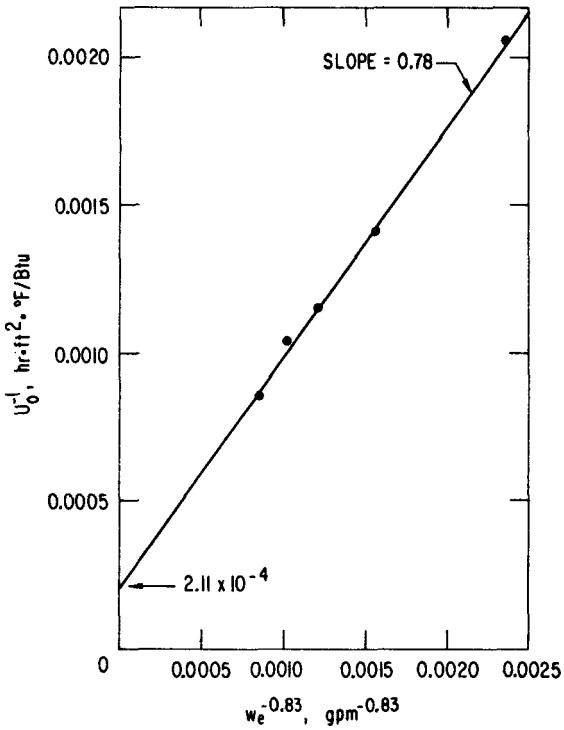

Fig. 11 Condenser Performance

5.4.2 Effects of Heat Flux

It is believed that the condensation process is in general gravity-controlled for the Trane heat exchanger. The interfacial shear caused by the downward flow of the ammonia vapor enhances the rate of condensation by reducing the effective thickness of the condensate film. The film Reynolds number at the bottom of the condenser

Table 5 Overall Heat-Transfer Coefficient as a Function of Water Flow Rate: Condenser

Water Flow Rate (gpm)	Heat Duty (10^6 Btu/h)	Rate of Condensation (lb/h)	Overall Heat-Transfer Coefficient (Btu/h·ft^2·°F)
3276	3.21 ± 0.07	6258 ± 65	870
3999			960
5034			1165
1463			485
2399			705
3161	2.42 ± 0.03	4577 ± 45	935
3986			1090
4997			1240
1472			540
2386			770
3174	4.16 ± 0.17	7847 ± 294	745
4017			850
5013			970
1468			445
2393			640

[a]These values can be converted to mean flow velocity (v ft/sec) using the relationship $v = 0.00233\ w_e$.

is in the range of 125 to 220, based on the total wetted perimeter assuming uniform liquid distribution -- this makes it a laminar-film condensation. According to Nusselt's analysis, the ammonia-side heat-transfer coefficient decreases as heat flux is increased. However, as Fig. 12 shows, a sharp drop in the ammonia-side coefficient is observed in the present study. The overall heat-transfer coefficient drops by about 20% as the heat flux is increased from 3150 Btu/h·ft^2 to 5300 Btu/h·ft^2. This significant drop is not anticipated in Nusselt's analysis for film condensation on a vertical surface. The observed decrease in U_o with increased heat flux could result from liquid flooding in the bottom of the heat exchanger.

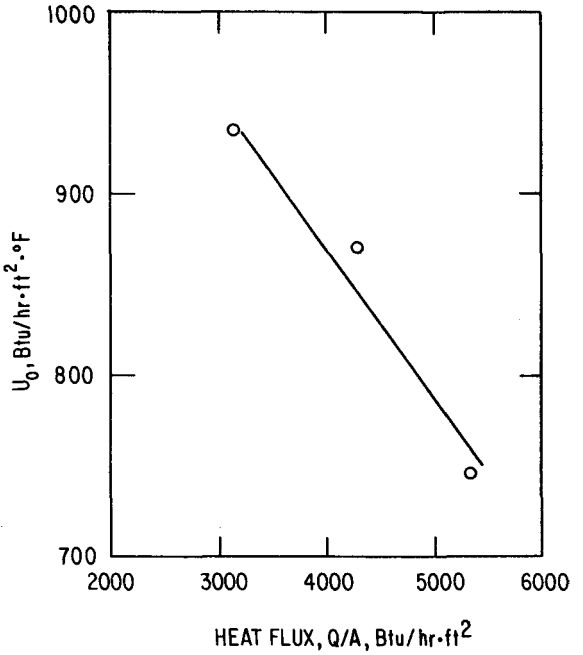

Fig. 12 Condenser Performance as a Function of Heat Flux

5.5 AMMONIA-SIDE PRESSURE DROP

The ammonia-side pressure drop does not directly affect the net power output from an OTEC plant because parasitic losses for the ammonia system are small compared to other parasitic losses. However, there is a net loss in the temperature driving force for a high ammonia-side pressure drop. Consequently, it is important to recognize that the ammonia-side pressure drop is negligible for a thin-film gravity-controlled evaporator operated in the falling-film mode. On the other hand, the pressure drop could be significant for an evaporator system in the forced-convection mode.

An analytical study by Yung et al.[8] indicates that the two-phase pressure drop for forced-convection evaporation in serrated-fin channels is a weak function of exit quality. Furthermore, it is nearly a linear function of the ammonia feed rates that were studied. The latter experimental data are presented in Fig. 13, and a linear curve is fitted through those points using a least-squares method.

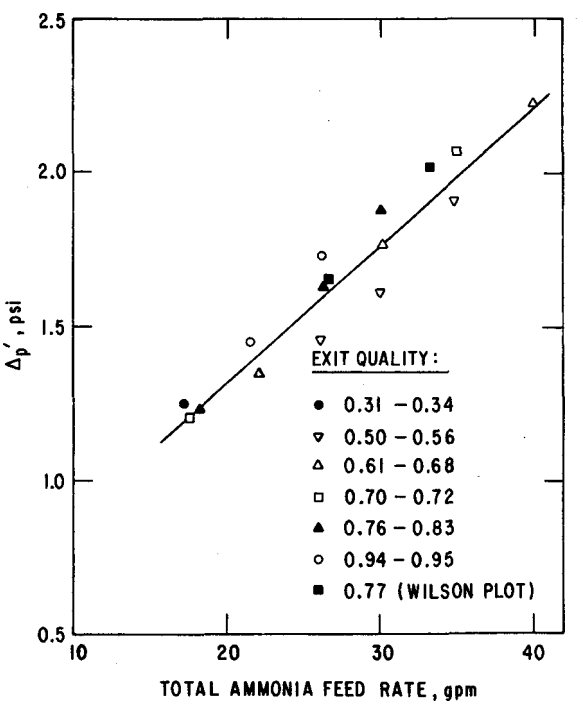

Fig. 13 Ammonia-Side Pressure Drop as a Function of Ammonia Feed Rate: Forced-Convection Mode

It should be borne in mind that the reported pressure drops include entrance and exit losses. These end losses are caused by a 90° turn in the flow direction at the inlet and outlet of the heat exchanger. According to Trane, these losses are about 0.2 psi at nominal conditions of 26 gpm and 77% exit quality.

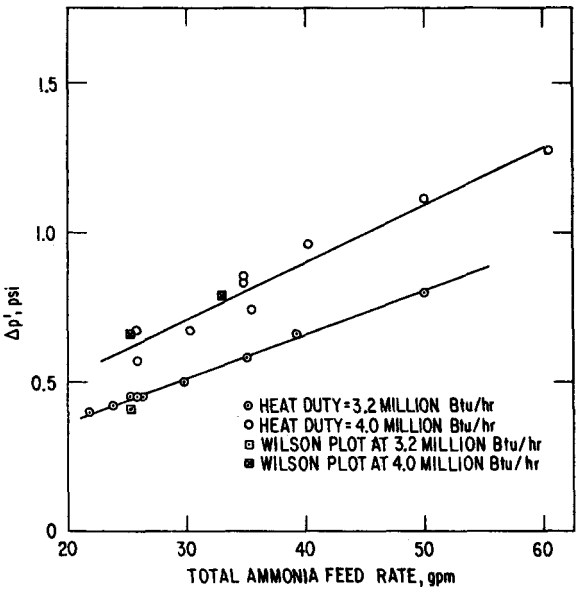

Fig. 14 Ammonia-Side Pressure Drop as a Function of Ammonia Feed Rate: Evaporator, Falling-Film Mode

The ammonia-side pressure drop in the falling-film evaporative mode is shown in Fig. 14. Figures 13 and 14 indicate that, for a given set of operating conditions, the pressure drop in the forced-convection mode is greater than that in the falling-film mode. At nominal conditions, the pressure drops in the forced-convection and falling-film modes are 1.6 psi and 0.4 psi, respectively. The pressure drop for a heat duty of 4 million Btu/h is about 35% greater than that for a heat duty of 3.2 million Btu/h at all ammonia feed rates. The 35% difference may be due to a higher ammonia-vapor feed rate at 4 million Btu/h heat duty. However, it is anticipated that the net pressure drop after accounting for the end losses should be comparatively small. Finally, the pressure drop for the condenser was negligibly small in the present range of study.

5.6 WATER-SIDE HEAT-TRANSFER COEFFICIENT AND PRESSURE DROP

Water-side heat-transfer coefficients were obtained from the Wilson-plot procedure and are shown in Fig. 15. However, no attempt has been made to compare these data with theoretical predictions because no reliable correlation was found in the literature for the compact heat exchanger. It is seen that the water-side coefficients for the evaporator in two modes of operation are in good agreement. As expected, h_i for the condenser is lower than that for the evaporator at the same feed rate.

Figure 16 shows water-side pressure drop for each of the two modes of evaporative operation. The pressure drops are proportional, within a few percent, to the square of the flow rate. No pressure-drop data were taken for the condenser because of instrumentation problems. However, Δp for the condenser is expected to be slightly greater than that for the evaporator.

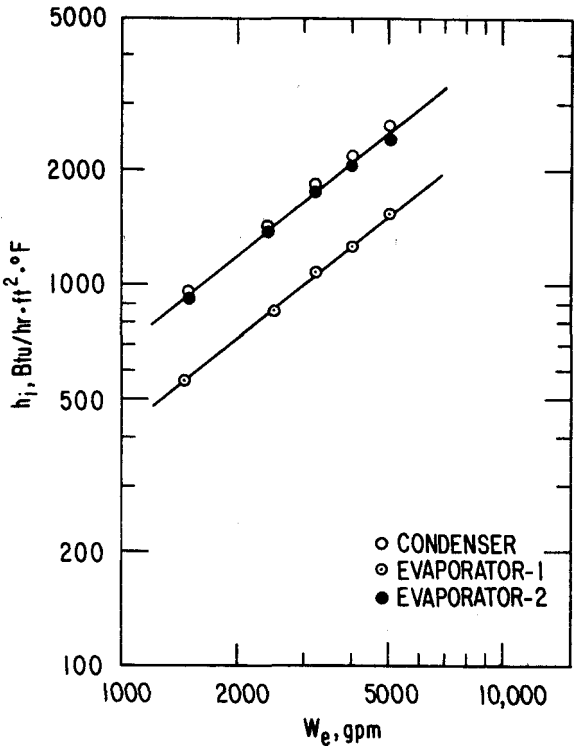

Fig. 15 Water-Side Heat-Transfer Coefficient as a Function of Water Flow Rate

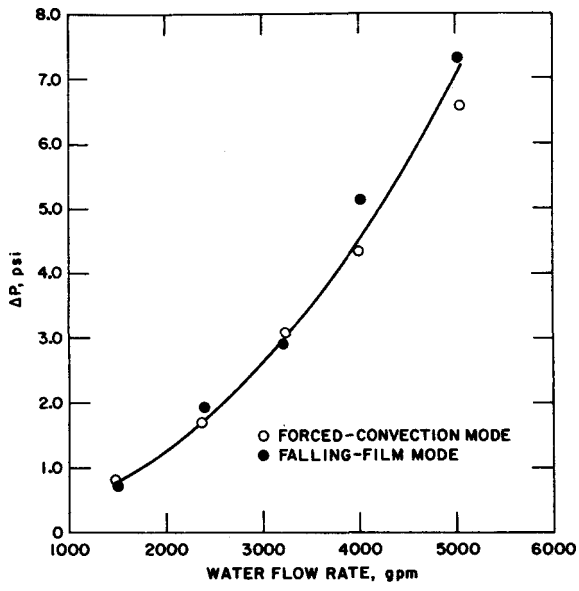

Fig. 16 Water-Side Pressure Drop As a Function of Water Flow Rate

6 ANALYTICAL MODELING

Analytical modeling of the two-phase flow and the heat transfer in serrated-fin channels has been reported by ANL.[8] The purpose of the present modeling effort was to improve the design methods of plate-fin evaporators and condensers for the OTEC program. The two-phase pressure drop and heat transfer were modeled using an annular-flow analysis for the laminar-film liquid phase. For the vapor phase, both annular-flow and turbulent-flow analyses were used, depending on the flow rate of the ammonia.

A flow controlled by interfacial shear was assumed for the forced-convection mode of evaporative operation. An annular flow controlled by gravity was assumed for the unit operated as a condenser. The unit was not analytically modeled as a falling-film evaporator, but the model can easily be modified to make such an analysis.

The theoretically predicted performance of the model was found to be in reasonably good agreement with the experimental test results reported here. The same model was applied to the data of Robertson[10] for convective vaporization of nitrogen. In the latter application, when the conditions included low mass fluxes and a negligible entrainment of liquid, reasonably good agreement was also found between theoretically predicted and experimentally determined results.

7 CONCLUSIONS

Based on the performance tests of the Trane plate-fin compact heat exchanger, the following conclusions can be drawn.

1. The measured overall heat-transfer coefficient was found to be stable and repeatable.
2. Fins on the ammonia-side act effectively in enhancing the heat-transfer performance of the forced-convection evaporative process.
3. The unit as presently designed has a liquid-distribution problem in the falling-film evaporative mode. It was observed that overall performance in that mode did not significantly improve on the overall performance of the unit in the forced-convection evaporative mode.
4. No significant enhancement due to the surface-tension (Gregorig) effect was observed for the condensation process. The serrated-fin arrangement, however, reduces the liquid condensate on the ammonia-side surfaces. Consequently, it gives a higher ammonia-side coefficient than can be obtained without a serrated arrangement.
5. The overall heat-transfer coefficient for the forced-convection mode is relatively insensitive to changes in ammonia-side operating conditions. On the other hand, U_o in the present range of study is quite sensitive to operating conditions when the unit is applied as a falling-film evaporator or as a condenser.

REFERENCES

1. Lewis, L.G., and N.F. Sather, *OTEC Performance Tests of the Union Carbide Flooded-Bundle Evaporator*, Argonne National Laboratory Report ANL/OTEC-PS-1 (Dec. 1978).

2. Yung, D.T., et al., *OTEC Performance Tests of the Union Carbide Enhanced-Tube Condenser*, Argonne National Laboratory Report ANL/OTEC-PS-2 (May 1979).

3. Hillis, D.L., et al., *OTEC Performance Tests of the Union Carbide Sprayed-Bundle Evaporator*, Argonne National Laboratory Report ANL/OTEC-PS-3 (May 1979).

4. Lewis, L.G., and N.F. Sather, *OTEC Performance Tests of the Carnegie-Mellon University Vertical Fluted-Tube Condenser*, Argonne National Laboratory Report ANL/OTEC-PS-4 (May 1979).

5. Lorenz, J.J., et al., *OTEC Performance Tests of the Carnegie-Mellon University Vertical Fluted-Tube Evaporator*, Argonne National Laboratory Report ANL/OTEC-PS-5 (July 1979).

6. Yung, D.T., et al., unpublished information, Argonne National Laboratory (1981).

7. Panchal, C.B., J.J. Lorenz, and D.L. Hillis; *The Effects of Ammonia Contamination by Water on OTEC Power-System Performance*, Argonne National Laboratory Report ANL/OTEC-PS-8 (Aug. 1981).

8. Yung, D.T., J.J. Lorenz, and C.B. Panchal; *Convective Vaporization and Condensation in Serrated-Fin Channels*, presented at the Winter ASME Meeting, Chicago (Nov. 1980).

9. Thomas, A., et al., *Experimental Tests of 1 MWt OTEC Heat-Exchangers*, Proc. 7th Ocean Energy Conversion Conf., Washington, D.C. (June 1980).

10. Robertson, J.M., *Boiling Heat Transfer with Liquid Nitrogen in Brazed-Aluminum Plate-Fin Heat Exchangers*, AIChE Symp. Series, Vol. 75, pp. 151-164 (1979).

ACKNOWLEDGMENTS

We acknowledge the contributions of the following persons: Anthony Thomas, manager of the OTEC Power System Development Program at Argonne; Floyd Davis of Globe Engineering, Lloyd Lewis and Chester Brzegowy of Argonne, for their work on the design and construction of the OTEC test facility; Oscar Despe for assistance with the data-handling equipment, Donald Hulet for supervising test facility operations; Ed O'Hare and Clarence Clark for assistance in carrying out the experiments; Mitchell Hulet for assistance in data reduction; John Cleland for editorial assistance; and Roberta Walker, Betty O'Meara, and Louise Benson for typing this report.

The following persons are gratefully acknowledged for their reviews of this report: Kenneth Bell, Oklahoma State University; Kenneth Read, U.S. Naval Academy; and Harry Foust, Trane Co.

APPENDIXES:

EXPERIMENTAL DATA

APPENDIX A:
UNIT OPERATED AS EVAPORATOR IN FORCED-CONVECTION MODE

Table A-1 Evaporator Performance in the Forced-Convection Mode, as a Function of Water Flow Rate over the Range of 1482-5043 gpm

Run No.	w_e (gpm)	q_e (10^6 Btu/h)	w'_e (gpm)	T_{ei} (°F)	T_{eo} (°F)	T'_e (°F)	U_o (Btu/h ft^2·°F)	$\Delta P'_e$ (psi)
1	3249	3.28	26.7	77.16	75.14	72.63	1236	1.67
2	2391	3.20	26.6	78.48	75.79	73.02	1041	1.65
3	3996	3.32	26.6	76.35	74.69	72.40	1404	1.65
4	5043	3.28	26.5	75.78	74.48	72.42	1589	1.62
5	1482	3.11	26.6	80.06	75.85	72.40	762	1.64

Table A-2 Evaporator Performance in the Forced-Convection Mode, as a Function of Water Flow Rate over the Range of 1502-5012 gpm

Run No.	w_e (gpm)	q_e (10^6 Btu/h)	w'_e (gpm)	T_{ei} (°F)	T_{eo} (°F)	T'_e (°F)	U_o (Btu/h ft^2·°F)	$\Delta P'_e$ (psi)
6	3203	4.08	33.2	79.76	77.21	74.17	1256	2.02
7	4015	4.01	33.2	79.22	77.22	74.45	1408	2
8	5012	3.98	33.2	78.49	76.90	74.34	1556	1.99
9	2407	4.05	33.1	81.30	77.93	74.52	1064	2.04
10	1502	3.97	33.1	83.88	78.58	74.36	785	2.03

Table A-3 Evaporator Performance in the Forced-Convection Mode, as a Function of Ammonia Feed Rate over the Range of 17-40 gpm

Run No.	w'_e (gpm)	q_e (106 Btu/h)	w_e (gpm)	T_{ei} (°F)	T_{eo} (°F)	T'_e (°F)	U_o (Btu/h ft^{2}·°F)	$\Delta p'_e$ (psi)
11	26.3	3.22	3245	76.69	74.71	72.26	1240	1.63
12	30	3.22	3244	76.77	74.77	72.31	1233	1.77
13	34.8	3.22	3246	77.00	75.01	72.59	1247	1.91
14	21.5	3.25	3246	76.78	74.77	72.24	1217	1.45
15	18.3	2.43	3248	75.65	74.15	72.28	1226	1.23
16	22.1	2.43	3245	75.80	74.30	72.39	1205	1.35
17	26.1	2.43	3246	75.86	74.36	72.43	1199	1.46
18	29.6	2.43	3246	76.05	74.55	72.66	1212	1.61
19	29.9	4	3244	78.09	75.62	72.65	1262	1.88
20	26.1	3.99	3246	78.11	75.65	72.54	1217	1.73
21	35	3.99	3246	78.21	75.75	72.46	1254	2.07
22	39.9	4	3247	77.92	75.45	72.46	1255	2.23
23	18	1.03	1540	77.03	75.70	74.45	723	1.22
24	17.2	0.92	3247	75.91	75.34	74.48	1054	1.25
25	17.6	2.04	1503	79.37	76.65	74.33	748	1.18
26	17.6	2.07	3254	77.27	75.99	74.31	1181	1.20

Table A-4 Water-Side Pressure Drop in a Forced-Convection Evaporator, as a Function of Water Flow Rate

w_e (gpm)	ΔP_e (psi)
1482	0.82
2392	2.69
3249	3.09
3996	4.33
5043	6.59

Table A-5 Ammonia Exit Quality and Two-Phase Pressure Drop in a Forced-Convection Evaporator, as Functions of Ammonia Feed Rate

Ammonia Feed Rate (gpm)	Heat Duty (10^6 Btu/h)	Ammonia Vapor Quality at Exit (%)	$\Delta P_e'$ (psi)
26.3	3.23 ± 0.4	76	1.63
30.1		66	1.77
34.8		56	1.91
21.5		94	1.45
18.3	2.43 ± 0.3	82	1.23
22.1		68	1.35
26.1		56	1.46
29.6		50	1.61
29.9	4 ± 0.2	83	1.88
26.1		95	1.73
35		70	2.07
39.9		61	2.23
17.2	0.92	31	1.25
17.6	2.07	72	1.20

APPENDIX B:
UNIT OPERATED AS EVAPORATOR IN FALLING-FILM MODE

Table B-1 Evaporator Performance in the Falling-Film Mode, as a Function of Water Flow Rate over the Range of 1501-5027 gpm

Run No.	w_e (gpm)	q_e (10^6 Btu/h)	w'_e (gpm)	T_{ei} (°F)	T_{eo} (°F)	T'_e (°F)	U_o (Btu/h ft^2·°F)	$\Delta P'_e$ (psi)
27	3216	3.18	25.6	77.32	75.34	72.29	1035	0.42
28	4017	3.25	25	76.86	75.24	72.31	1138	0.44
29	5027	3.22	24.8	76.43	75.15	72.36	1225	0.42
30	2403	3.24	25.8	78.54	75.84	72.35	888	0.42
31	1501	3.22	25.9	80.95	76.64	72.35	671	0.41
32	3211	3.20	25.7	77.37	75.37	72.37	1056	0.37

Table B-2 Evaporator Performance in the Falling-Film Mode, as a Function of Water Flow Rate over the Range of 1498-5017 gpm

Run No.	w_e (gpm)	q_e (10^6 Btu/h)	w'_e (gpm)	T_{ei} (°F)	T_{eo} (°F)	T'_e (°F)	U_o (Btu/h ft^2·°F)	$\Delta P'_e$ (psi)
33	3201	4.01	33.1	78.12	75.61	72.29	1162	0.76
34	3996	3.99	32.8	77.58	75.58	72.54	1302	0.78
35	4999	3.98	33	76.91	75.32	72.52	1451	0.75
36	2401	4.05	33	76.68	76.30	72.60	1004	0.83
37	1498	4	33	82.40	77.04	72.47	747	0.84
38	3198	3.98	33.1	78.07	75.58	72.33	1173	0.79
39	3198	4	25.4	78.75	76.24	72.20	992	0.65
40	4020	3.99	25.2	77.90	75.91	72.19	1108	0.65
41	5017	4.02	25.1	77.48	75.87	72.34	1211	0.67
42	2403	4.03	25.7	80.55	77.19	72.69	863	0.68
43	1518	4.04	25.7	83.28	77.95	72.24	645	0.67
44	3203	3.99	25.7	78.83	76.33	72.39	1010	0.62

Table B-3 Evaporator Performance in the Falling-Film Mode, as a Function of the Recirculation Ratio of the Ammonia

Run No.	Recirculation Ratio	q_e (10^6 Btu/h)	w_e (gpm)	w'_e (gpm)	T_{ei} (°F)	T_{eo} (°F)	T_e (°F)	U_o (Btu/h ft^2·°F)	ΔP_e (psi)
45	0.31	3.20	3221	25.8	77.32	75.35	72.61	1044	0.45
46	0.42	3.20	3222	23.7	77.52	75.53	72.30	995	0.42
47	0.40	3.22	3220	21.8	77.77	75.77	72.29	943	0.40
48	0.45	3.19	3221	25.3	77.36	75.38	72.32	1032	0.45
49	0.51	3.20	3221	29.6	77.08	75.09	72.32	1120	0.50
50	0.79	3.20	3220	34.9	77.05	75.06	72.48	1185	0.58
51	1.02	3.22	3220	39.3	77.03	75.02	72.49	1209	0.66
52	0.32	3.22	3221	26.2	77.47	75.47	72.44	1053	0.45
53	1.63	3.19	3222	49.9	77.01	75.02	72.53	1216	0.80
54	0.04	3.99	3203	25.8	78.83	76.33	72.39	1014	0.57
55	0.45	4	3190	35.6	78.26	75.74	72.50	1177	0.74
56	0.23	4	3195	30.3	78.32	75.81	72.41	1137	0.67
57	0.03	4.03	3195	25.8	78.70	76.17	72.32	1037	0.67
58	0.41	4.02	3195	34.8	78.44	75.92	72.74	1202	0.85
59	0.64	4.01	3196	40.2	77.95	75.44	72.37	1235	0.96
60	1.09	3.96	3194	50	77.95	75.47	72.49	1250	1.11
61	0.42	3.99	3196	34.8	78.03	75.52	72.35	1178	0.84
62	1.52	4.03	3197	60.6	78.28	75.75	72.63	1244	1.27

Table B-4 Two-Phase Pressure Drop of Ammonia in a Falling-Film Evaporator, as a Function of Ammonia Feed Rate

Ammonia Feed Rate (gpm)	Heat Duty (10^6 Btu/h)	$\Delta P_e'$ (psi)
25.8	3.20 ± .03	0.45
23.7		0.42
21.8		0.40
25.3		0.45
29.6		0.50
34.9		0.58
39.3		0.66
26.2		0.45
50		0.80
25.8	4 ± .11	0.57
35.6		0.74
30.3		0.67
25.8		0.67
34.8		0.85
40.2		0.96
50		1.11
34.8		0.84
60.6		1.27

APPENDIX C:
UNIT OPERATED AS CONDENSER

Table C-1 Condenser Performance as a Function of Water Flow Rate over the Range of 1463-5034 gpm

Run No.	w_c (gpm)	q_c (10^6 Btu/h)	T_{ci} (°F)	T_{co} (°F)	T'_c (°F)	U_o (Btu/h ft^2·°F)	$\Delta p'_c$ (psi)
63	3276	3.33	42.62	44.64	48.57	872	-0.03
64	3999	3.34	42.45	44.12	47.81	962	-0.01
65	5034	3.32	42.23	43.60	46.84	1133	0.10
66	1463	3.30	42.62	47.12	53.82	486	0.06
67	2399	3.28	42.10	44.83	49.57	707	0.02

Table C-2 Condenser Performance as a Function of Water Flow Rate over the Range of 1472-4997 gpm

Run No.	w_c (gpm)	q_c (10^6 Btu/h)	T_{ci} (°F)	T_{co} (°F)	T'_c (°F)	U_o (Btu/h ft^2·°F)	$\Delta p'_c$ (psi)
68	3161	2.44	42.15	43.70	46.35	935	0.05
69	3986	2.43	41.85	43.06	45.38	1088	0.06
70	4997	2.44	42.22	43.19	45.28	1242	0.07
71	1472	2.41	42.50	45.76	50.03	541	0.08
72	2386	2.40	41.94	43.95	47.05	772	0.03

Table C-3 Condenser Performance as a Function of Water Flow Rate over the Range of 1468-5013 gpm

Run No.	w_c (gpm)	q_c (10^6 Btu/h)	T_{ci} (°F)	T_{co} (°F)	T'_c (°F)	U_o (Btu/h ft^2·°F)	$\Delta p'_c$ (psi)
73	3174	4.15	42.41	45.02	50.96	747	0.23
74	4017	4.18	42.47	44.55	49.92	849	0.23
75	5013	4.24	42.81	44.49	49.33	969	0.24
76	1468	4.21	42.19	47.92	57.49	445	0.23
77	2393	4	42.26	45.59	52.08	641	0.25